SCISPACE
formerly Typeset

Open access • Journal Article • DOI:10.1063/1.474145

Quantum study of the Li+HF→LiF+H reaction — Source link

Alfredo Aguado, Miguel Paniagua, Manuel Lara, Octavio Roncero

Published on: 15 Dec 1997 - Journal of Chemical Physics (American Institute of Physics)

Topics: Potential energy surface, Jacobi coordinates, Energy profile, Reaction dynamics and Kinetic energy

Related papers:

- Quantum stereodynamics of the Li HF v,j reactive collision for different initial states of the reagent
- A detailed three-dimensional quantum study of the Li+FH reaction
- Study of the reaction dynamics of Li+HF, HCl by the crossed molecular beams method
- Potential energy surface and wave packet calculations on the Li+HF→LiF+H reaction
- Three-dimensional quantum mechanical study of the Li+HF→LiF+H process: Calculation of integral and differential cross sections

Share this paper:

View more about this paper here: https://typeset.io/papers/quantum-study-of-the-li-hf-lif-h-reaction-4ghiq5fvs0

Global potential energy surfaces for the H3+ system. Analytical representation of the adiabatic ground-state 11A′ potential

Alfredo Aguado, Octavio Roncero, César Tablero, Cristina Sanz, and Miguel Paniagua

Citation: J. Chem. Phys. **112**, 1240 (2000); doi: 10.1063/1.480539
View online: http://dx.doi.org/10.1063/1.480539
View Table of Contents: http://jcp.aip.org/resource/1/JCPSA6/v112/i3
Published by the American Institute of Physics.

Additional information on J. Chem. Phys.

Journal Homepage: http://jcp.aip.org/
Journal Information: http://jcp.aip.org/about/about_the_journal
Top downloads: http://jcp.aip.org/features/most_downloaded
Information for Authors: http://jcp.aip.org/authors

ADVERTISEMENT

Downloaded 15 Mar 2013 to 161.111.22.69. Redistribution subject to AIP license or copyright; see http://jcp.aip.org/about/rights_and_permissions

Global potential energy surfaces for the H_3^+ system. Analytical representation of the adiabatic ground-state $1\,^1A'$ potential

Alfredo Aguado[a] and Octavio Roncero
Instituto de Matemáticas y Física Fundamental, C.S.I.C., Serrano 123, 28006 Madrid, Spain

César Tablero, Cristina Sanz, and Miguel Paniagua[b]
Departamento de Química Física, Facultad de Ciencias C-XIV, Universidad Autónoma de Madrid, 28049 Madrid, Spain

(Received 5 August 1999; accepted 19 October 1999)

Adiabatic global potential energy surfaces, for singlet and triplet states of A' and A'' symmetries, were computed for an extensive grid for a total of 8469 conformations of H_3^+ system at full configuration interaction *ab initio* level and using an extended basis set that has also been optimized for excited states. An accurate (root-mean-square error lower than 20 cm^{-1}) global fit to the ground-state potential is obtained using a diatomics-in-molecules approach corrected by several symmetrized three-body terms with a total of 96 linear parameters and 3 nonlinear parameters. This produces an accurate global potential which represents all aspects of ground-state H_3^+ including the absolute minimum, the avoided crossing and dissociation limits, satisfying the correct symmetry properties of the system. The rovibrational eigenstates have been calculated up to total angular momentum $J=20$ using hyperspherical coordinates with symmetry adapted basis functions. The infrared spectra thus reproduced is within 1 cm^{-1} with respect to the experimental values for several transitions. © *2000 American Institute of Physics.* [S0021-9606(00)00803-5]

I. INTRODUCTION

Ion–molecule reactions are of great importance in gas phase environments such as molecular hydrogen plasmas occurring in interstellar clouds, planetary ionospheres, ion sources, and thermonuclear experiments. A very important reaction in the interstellar medium is the prototype reaction[1]

$$H_2^+ + H_2 \rightarrow H_3^+ + H,$$

forming H_3^+, which is a major cation in hydrogen plasmas and plays an important role, due to its simplicity, as a benchmark system for high accuracy *ab initio* molecular theory and reaction dynamics. Full reviews of the experimental and theoretical work on H_3^+ have been presented by McNab[2] and Tennyson.[3] New interest has arisen in highly rotationally excited states of H_3^+ motivated by the experimental investigations of the extraordinarily complex IR predissociation spectrum—almost 27 000 lines over the range 872 to 1094 cm^{-1}, grouped into four separated peaks when considering a pseudo-low-resolution spectrum—by Carrington and Kennedy.[4] Clary[5] has suggested that rotational effects play a key role in explaining the temperature dependence of ion–molecule reactions, especially at the low interstellar temperatures.

Very accurate H_3^+ electronic structure calculations in the near equilibrium geometry have been reported.[6] Local potential energy surfaces (LPES) on the highest level of sophistication have appeared recently,[7,8] but covering only 69 points on the minimum region of the ground-state potential energy surface, based on previous full configuration interaction (FCI) calculations due to Meyer *et al.* (the so-called MBB LPES).[9] Dinelli *et al.*,[10] using high-resolution spectroscopic data for H_3^+, H_2D^+, D_2H^+, and D_3^+, have determined effective mass-dependent LPES for each isotopomer. These potential surfaces are expressed as a sum of the mass-independent Born–Oppenheimer potential and a mass-dependent adiabatic correction. Unfortunately, the study of highly rotationally excited states near dissociation,[11] with a high density of long-lived metastable levels lying in the continuum, above the lowest H_2+H^+ dissociation limit (and indeed maybe lying above higher dissociation limits corresponding to fragment H_2 molecules in higher rotational, or even vibrational, levels),[12] is impossible to do with LPES because their validity is only for energies below the lowest dissociation limit.

Despite the high symmetry and electronic simplicity—two-electron system—of the H_3^+ ion, only a few *ab initio* FCI calculations of the global potential energy surfaces (GPES), including the correct behavior as the molecule dissociates and for all possible geometrical configurations, have been reported for ground ($1\,^1A'$[13,14]) and excited ($1\,^3\Sigma_u^+$,[15] $2\,^1A'$[14]) states and for a maximum of 680 different spatial geometries. This fact contrasts with very accurate GPES obtained for more complex polyatomics such as H_3, with more than 8000 different spatial geometries,[16] H_2O,[17,18] H_2F,[19] or H_4,[20] to name just a few. Moreover, in a recent paper concerning a first attempt on a calculated spectrum for near-dissociation H_3^+, Henderson and Tennyson conclude that, in the absence of a high quality global potential, an attack on the global H_3^+ problem would be very worthwhile and is easily within the range of present methods.[21] In this paper we

[a]Present address: Departamento de Química Física, Facultad de Ciencias C–XIV, Universidad Autónoma de Madrid, 28049 Madrid, Spain.
[b]Electronic mail: miguel.paniagua@uam.es

 © 2000 American Institute of Physics

Downloaded 15 Mar 2013 to 161.111.22.69. Redistribution subject to AIP license or copyright; see http://jcp.aip.org/about/rights_and_permissions

present FCI calculations for the global H_3^+ system including 8469 different spatial geometries and, for each geometry, we compute a total of 36 states of A' and A'' irreducible representations with both singlet and triplet multiplicities.

There are several global analytical representations of the adiabatic ground-state $1\,^1A'$ potential for H_3^+ in the literature.[13,22,23] However, all of these GPES are unsatisfactory for several reasons: the diatomics-in-molecules (DIM) surface of Preston and Tully,[22] which is the most widely used in trajectory calculations, is qualitatively correct; it was the first study of the avoided crossing due to the presence of two dissociation channels, $H_2(^1\Sigma_g^+)+H^+$ and $H_2^+(^2\Sigma_u^+)+H$, but it is not accurate even at low energies; the Schinke *et al.* GPES[13] is based on their *ab initio* calculations but the functional form used has discontinuous derivatives and contains unphysically deep minima for certain regions, probably due to the small number of *ab initio* points. The most recent GPES of Prosmiti *et al.*[23] is a combination of two potential forms using the energy switching approach of Varandas[24] to connect them. The first potential form, corresponding to the Born–Oppenheimer portion of the Dinelli *et al.* LPES,[10] reproduces the spectroscopic measurements with quantitative accuracy and is reliable for the minimum region of the global potential. The second potential form is represented by two terms, a short-range 32 parameters fit to 327 data points of Schinke *et al.* (with a standard deviation of about 280 cm^{-1}) plus a long-range term to describe the charge-induced dipole and charge-quadrupole contributions obtained from perturbation theory. Unfortunately, this latter term does not reflect the symmetry of H_3^+ causing the global potential to contain unphysical behavior with respect to symmetry. In addition, the connection regions between the two potentials of very different accuracy may also be a problem for dynamical calculations.

The construction of an accurate GPES covering the whole configuration space up to and above dissociation, for the ground-state H_3^+ system, remains an important problem. In fact, the most recent dynamical study of this system using a quantum-mechanical approach[25] is based on the very approximate DIM GPES.[22] Moreover, in a first attempt to obtain a calculated spectrum for near-dissociation H_3^+,[21] Henderson and Tennyson have used the MBB LPES[9] that lacks any representation of the regions near dissociation. In this paper we also present a global analytical representation of the adiabatic ground-state $1\,^1A'$ potential for the H_3^+ system. Moreover, we have calculated the rovibrational levels of the ground-state H_3^+ system, using symmetry adapted basis functions in hyperspherical coordinates. The use of symmetry as well as an iterative Lanczos procedure allowed us to calculate levels up to an energy of about 14000 cm^{-1} and with high angular momentum ($J=20$). The results thus obtained are used to check the accuracy of the GPES reported here, by comparison with the experimental infrared spectra as well as with previous theoretical studies of spectroscopic accuracy.

II. POTENTIAL ENERGY CALCULATIONS

The construction of a reliable GPES faces the problem that the absolute error of the energies, calculated with variational or perturbative procedures, is large. For the H_3^+, a full configuration interaction (FCI) solution is trivial and nowadays it is possible to do the computational effort needed to obtain several thousands of FCI energies with an extended basis set. The single best FCI energy obtained for the H_3^+ minimum[9] is about 95 cm^{-1} higher than the very accurate result reported recently.[26,7]

Nevertheless, when constructing a GPES, we are not interested in total energies but in energy differences, which are usually small quantities. In forming the difference between two large quantities of similar size, we must consider that errors at each term of the difference are similar and will cancel to a large extent, with a final result for the difference that may have a lower error (with respect to the exact difference) than the absolute error obtained in the calculated total energy. Usually, the error in the energy differences involving electronic excited states increases with respect to that obtained for the ground state. This is due to the fact that basis sets are optimized, in general, for atomic ground state that correlate with molecular ground state and several molecular excited states. If we compute molecular excited states correlating with atomic excited states, then we need atomic basis sets optimized for both atomic ground state and several excited states.

In order to assess the relative accuracy which can be expected using different basis sets, we begin by comparing results of calculations for H_2. We report FCI calculations obtained using the $(10s4p2d)/[7s4p2d]$ basis of Meyer, Botschwina, and Burton (MBB)[9] and a new basis set $(11s6p2d)/[8s6p2d]$ obtained from the MBB basis set which is further augmented by a single s function with exponent 0.012 649 8, that has been optimized with respect to the energy of the hydrogen $2s$ orbital, and two sets of p functions with exponents 0.045 557 6 and 0.017 773 8, that have been optimized with respect to the energy of the hydrogen $2p$ orbitals. Figures 1 and 2 display errors in energy differences as a function of the internuclear distance (taking as reference the H_2 ground-state minimum energy), for singlet states and triplet states, respectively. We have taken as the exact energy differences those obtained from the most accurate potential curves for each state considered[27] (labeled $X\,^1\Sigma_g^+$, E, $F\,^1\Sigma_g^+$, $B\,^1\Sigma_u^+$, $B'\,^1\Sigma_u^+$, $C\,^1\Pi_u$ in Fig. 1 and $a\,^3\Sigma_g^+$, $b\,^3\Sigma_u^+$, $e\,^3\Sigma_u^+$, $i\,^3\Pi_g$ in Fig. 2).

From Fig. 1 we can see that errors in energy differences are very similar for the ground state ($X\,^1\Sigma_g^+$) using both basis sets (see the upper panel for present results and the lower panel for MBB results). The same behavior is observed in Fig. 2 for errors corresponding to the $b\,^3\Sigma_u^+$ excited state that are very similar for both basis sets. These are the only two states ($X\,^1\Sigma_g^+$ and $b\,^3\Sigma_u^+$) of H_2 having as asymptotic limits $H(1s)+H(1s)$. However, if we compare errors in energy differences for any other H_2 excited state, with different asymptotic limits, we can see a general worse behavior for MBB basis set in both figures (several states fall out of the limits in both figures for all internuclear distances using the MBB basis set). Moreover, in Fig. 1 we can see that errors corresponding to the H_2 ground state ($X\,^1\Sigma_g^+$) are lower than 20 cm^{-1} for distances between approximately 1.0

Downloaded 15 Mar 2013 to 161.111.22.69. Redistribution subject to AIP license or copyright; see http://jcp.aip.org/about/rights_and_permissions

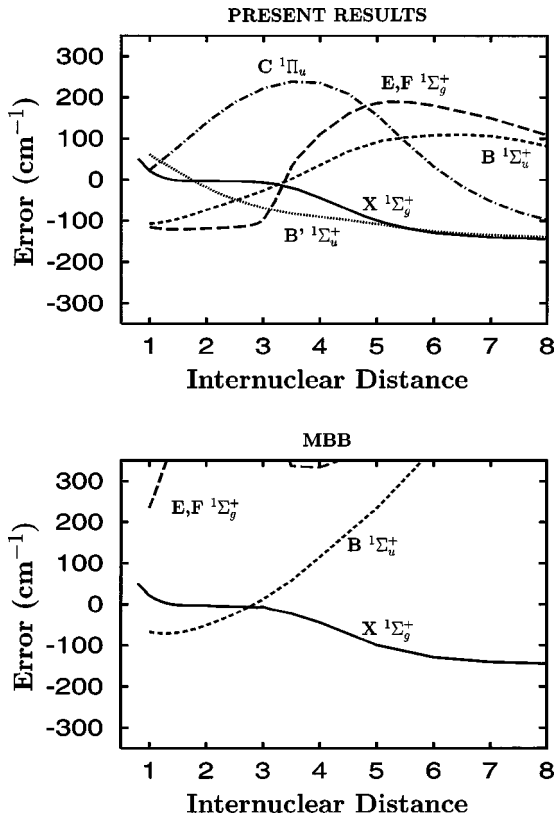

FIG. 1. Errors in energy differences for different singlet states of the H_2 molecule as a function of the internuclear distance. Errors in cm^{-1} and distances in atomic units. Upper panel corresponds to present results and lower panel corresponds to Meyer *et al.* (Ref. 9) results.

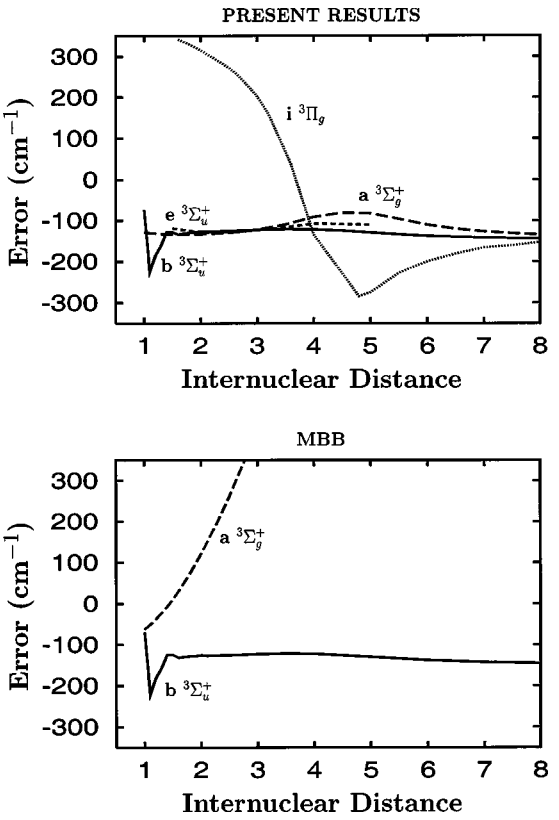

FIG. 2. Errors in energy differences for different triplet states of the H_2 molecule as a function of the internuclear distance. Units and panels as in Fig. 1.

and 3.5 atomic units, corresponding to the potential well region. From Fig. 1 we can see that the error at dissociation for the H_2 ground state ($X\,^1\Sigma_g^+$) is about 145 cm^{-1}; this dissociation error affects the remaining error curves as we can clearly see for several triplet states in Fig. 2 (see $a\,^3\Sigma_g^+$, $b\,^3\Sigma_u^+$, and $e\,^3\Sigma_u^+$, upper panel), which show very stable error curves but displaced from zero error in about 145 cm^{-1}. If we compute these error curves with respect to their own minima, the resulting curves are all around the zero value error in energy differences.

We have carried out a similar study for the ground state ($X\,^2\Sigma_g^+$) and several excited states ($2\,^2\Sigma_g^+$, $1\,^2\Sigma_u^+$, $2\,^2\Sigma_u^+$, $1\,^2\Pi_u$, $1\,^2\Pi_g$) of the H_2^+. In the upper panel of Fig. 3 the errors in energy differences for all the mentioned doublet states are compared with the exact energy differences. The latter have been obtained from the exact potential energy curves.[28] The corresponding results using the MBB basis set have been plotted in the bottom panel of Fig. 3. As for the H_2 system, there are several states ($1\,^2\Pi_u$, $1\,^2\Pi_g$) that fall out of the figure using the same energy scale as that used for our results. Moreover, using the MBB basis set, only two states ($X\,^2\Sigma_g^+$ and $1\,^2\Sigma_u^+$, see the bottom panel in Fig. 3) are in error lower than 20 cm^{-1} in the region of the potential well, while when using the basis set proposed in this paper all the states except $1\,^2\Pi_u$ fulfill this condition. Finally, one important difference with respect to H_2 is that for H_2^+ we have a very low error for dissociation.

Using the $(11s6p2d)$ basis set, with the four innermost s functions contracted to $[8s6p2d]$, the total energy of H_3^+ at its ground-state equilibrium geometry (equilateral triangle, equilibrium bond length $R_e = 1.6500$ a.u.) is $-1.343\,100$ a.u., about 161 cm^{-1} above the exact energy.[7,26] However, as we have stressed above, this absolute error is not as important as the error in energy differences with respect to a reference zero energy. Since we have computed the very accurate 69 points quoted recently by Cencek *et al.*,[7] it is possible to obtain a root-mean-square (rms) deviation of our energy differences errors, taken as zero energy value the corresponding energy of the equilibrium geometry both for our energy differences (zero energy at $-1.343\,100$ a.u.) as for the exact energy differences (zero energy at $-1.343\,835$ a.u.). The resulting rms deviation is less than 17 cm^{-1}. Therefore, the expected rms errors for the H_3^+ ground-state well and its dissociation channels, $H_2(X\,^1\Sigma_g^+) + H^+$ and $H(1s) + H_2^+(X\,^2\Sigma_g^+)$, are about 20 cm^{-1}. Only the full dissociation region of the H_3^+ ground-state GPES $[H(1s) + H(1s) + H^+]$ is expected to yield a higher error, growing smoothly to a maximum value of 145 cm^{-1} as the internuclear separations increase.

We use the $(11s6p2d)/[8s6p2d]$ basis set to compute the final FCI data points for a total of 8469 different H_3^+ conformations. We have used symmetry group C_s for all the geometries and we have computed 36 different states at each point as follows: $9\,^1A'$, $9\,^1A''$, $9\,^3A'$ and $9\,^3A''$. To specify our grids of H_3^+ conformations, we have adopted the coordinates used by Boothroyd *et al.*[16] in a refined H_3 potential energy surface. These coordinates can be described by the

Downloaded 15 Mar 2013 to 161.111.22.69. Redistribution subject to AIP license or copyright; see http://jcp.aip.org/about/rights_and_permissions

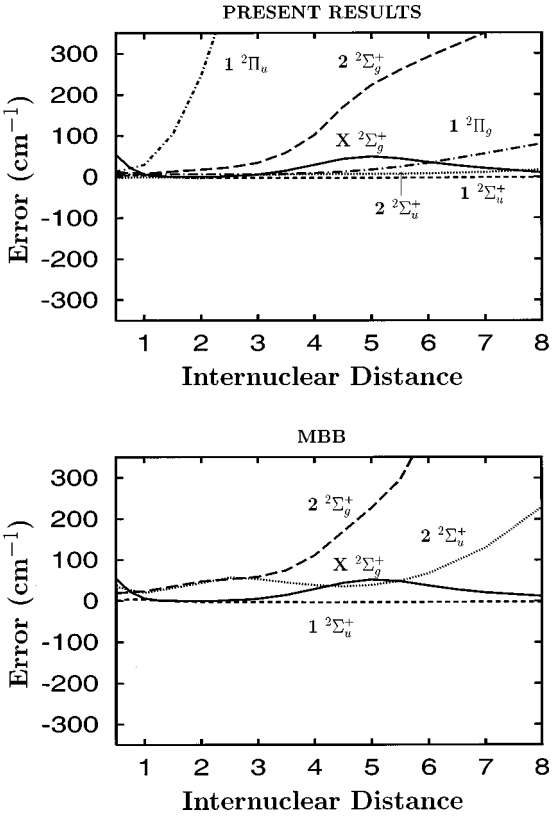

FIG. 3. Errors in energy differences for different doublet states of the H_2^+ molecule as a function of the internuclear distance. Units and panels as in Fig. 1.

shortest interatomic distance r_1, the next-shortest distance r_2, and the exterior angle between them, θ.

We have used the preliminary grid described by Boothroyd *et al.*[16] that comprised 540 conformations. Moreover, we have used also the more comprehensive grid that was specified as follows: r_1 and r_2 were chosen from 0.6 to 2.0 a_0 in increments of 0.1 a_0 ($1a_0=0.529\,177$ Å), also for 2.15, 2.3, 2.45, 2.6, 2.8, 3.0, 3.2, 3.4, 3.7, 4.0, 4.3, 4.6, 5.0, and 5.5 a_0, such that $r_1 \leqslant r_2 \leqslant r_3$; θ ran from 0° to 90° inclusive in increments of 10° and continued from $\theta=90°$ to $\theta \leqslant 120°$ in one, two, or three equally spaced increments that did not exceed 10°. More conformations have been added to the ''comprehensive'' grid as described by Boothroyd *et al.*[16] totalizing 6548 conformations. Some of them are coincident with the preliminary grid.

We have added conformations corresponding to the H_3 van der Waals region,[29] filling in a region at large H–H_2 distances from 5.5 to 15.0 a_0 with r_1 chosen from 0.7 to 4.0 a_0. The total number of different conformations was 7995 including the van der Waals grid.

Finally, we include a grid of conformations that are very close equilateral triangles (close to the D_{3h} minimum region) that we specify as follows: r_1 and r_2 were chosen from 1.61 to 1.69 a_0 in increments of 0.01 a_0 such that $r_1 \leqslant r_2$; θ ran from 56° to 64° inclusive in increments of 1°, totalizing 405 different conformations. If we add to all of these conformations the 69 proposed by Meyer *et al.*[9] and used by Cencek *et al.*[7] in their very accurate H_3^+ ground-state calculations, we obtain a total number of 8469 conformations and 36 FCI energy values for each one (304 884 energy values that we do not quote here for obvious reasons). A file containing the 8469 ground-state H_3^+ data points used to obtain the GPES reported in this paper has been placed in the electronic depository EPAPS.[30]

III. THE GROUND-STATE H_3^+ GLOBAL SURFACE

We write the global potential energy surface corresponding to the H_3^+ ground state ($1\,^1A'$) as

$$V_{H_3^+}=V_{\mathrm{DIM}}+\sum_{L}^{\mathrm{LMAX}} V_{ABC}^{(3)L}(R_{AB},R_{AC},R_{BC}), \tag{1}$$

where V_{DIM} in Eq. (1) is the lowest eigenvalue of the symmetric 3×3 matrix, corresponding to the diatomics-in-molecules approach with neglected overlap, given by

$$\begin{aligned}
H_{11}&=V_{AB}^{(2)}(H_2,{}^1\Sigma_g^+)-2V_H^{(1)}+\tfrac{1}{2}[V_{AC}^{(2)}(H_2^+,{}^2\Sigma_g^+)\\
&\quad+V_{AC}^{(2)}(H_2^+,{}^2\Sigma_u^+)+V_{BC}^{(2)}(H_2^+,{}^2\Sigma_g^+)\\
&\quad+V_{BC}^{(2)}(H_2^+,{}^2\Sigma_u^+)],\\
H_{22}&=V_{AC}^{(2)}(H_2,{}^1\Sigma_g^+)-2V_H^{(1)}+\tfrac{1}{2}[V_{AB}^{(2)}(H_2^+,{}^2\Sigma_g^+)\\
&\quad+V_{AB}^{(2)}(H_2^+,{}^2\Sigma_u^+)+V_{BC}^{(2)}(H_2^+,{}^2\Sigma_g^+)\\
&\quad+V_{BC}^{(2)}(H_2^+,{}^2\Sigma_u^+)],\\
H_{33}&=V_{BC}^{(2)}(H_2,{}^1\Sigma_g^+)-2V_H^{(1)}+\tfrac{1}{2}[V_{AB}^{(2)}(H_2^+,{}^2\Sigma_g^+)\\
&\quad+V_{AB}^{(2)}(H_2^+,{}^2\Sigma_u^+)+V_{AC}^{(2)}(H_2^+,{}^2\Sigma_g^+)\\
&\quad+V_{AC}^{(2)}(H_2^+,{}^2\Sigma_u^+)],\\
H_{12}&=\tfrac{1}{2}[V_{BC}^{(2)}(H_2^+,{}^2\Sigma_u^+)-V_{BC}^{(2)}(H_2^+,{}^2\Sigma_g^+)],\\
H_{13}&=\tfrac{1}{2}[V_{AC}^{(2)}(H_2^+,{}^2\Sigma_u^+)-V_{AC}^{(2)}(H_2^+,{}^2\Sigma_g^+)],\\
H_{23}&=\tfrac{1}{2}[V_{AB}^{(2)}(H_2^+,{}^2\Sigma_u^+)-V_{AB}^{(2)}(H_2^+,{}^2\Sigma_g^+)],
\end{aligned}$$

$V_H^{(1)}$ being the energy of the ^2S state of H($1s$) atom (-0.5 a.u. or $-109\,737$ cm^{-1}).

The two-body energies $V_{AB}^{(2)}$ (including the nuclear repulsion), may be written as a sum of two terms

$$V_{AB}^{(2)}=V_{\mathrm{short}}+V_{\mathrm{long}}, \tag{2}$$

where V_{short} prevails for small internuclear distances (the short range of the potential), which must fulfill the next condition

$$\lim_{R_{AB}\to0} V_{AB}^{(2)}=\lim_{R_{AB}\to0} V_{\mathrm{short}}\to\infty.$$

A simple alternative is to choose for V_{short} the shielded Coulomb potential

$$V_{\mathrm{short}}=c_0\frac{e^{-\alpha R_{AB}}}{R_{AB}}, \quad (\alpha,c_0>0). \tag{3}$$

We choose for V_{long} an expansion of order I

$$V_{\mathrm{long}}=\sum_{i=1}^{I} c_i\rho_{AB}^i, \tag{4}$$

Downloaded 15 Mar 2013 to 161.111.22.69. Redistribution subject to AIP license or copyright; see http://jcp.aip.org/about/rights_and_permissions

TABLE I. Two-body[a] term $V^{(2)}(H_2,\ ^1\Sigma_g^+)$.

i	c_i
0	0.101 395 751(+01)
1	−0.526 324 017(+01)
2	0.125 893 268(+03)
3	−0.338 282 397(+04)
4	0.709 290 230(+05)
5	−0.107 000 112(+07)
6	0.113 271 582(+08)
7	−0.828 291 974(+08)
8	0.408 176 908(+09)
9	−0.129 107 831(+10)
10	0.236 346 508(+10)
11	−0.190 174 039(+10)
α_{HH}	0.192 102 300(+01)
$\beta^{(2)}_{HH}$	0.177 626 800(+01)

[a]All the coefficients are given in atomic units.

TABLE III. Two-body[a] term $V^{(2)}(H_2^+,\ ^2\Sigma_u^+)$.

i	c_i
0	0.365 653 648(+03)
1	0.139 647 152(+01)
2	−0.161 982 515(+02)
3	0.606 990 392(+03)
4	−0.133 254 221(+05)
5	0.189 935 494(+06)
6	−0.177 898 791(+07)
7	0.110 321 235(+08)
8	−0.447 664 035(+08)
9	0.114 117 310(+09)
10	−0.165 634 015(+09)
11	0.104 351 423(+09)
α_{HH^+}	0.938 759 600(+01)
$\beta^{(2)}_{HH^+}$	0.112 172 600(+01)

[a]All the coefficients are given in atomic units.

in functions ρ_{AB} fulfilling that V_{long} tends to zero when the internuclear distance R_{AB} tends to zero or to infinity. Although the first condition is not strictly necessary, it allows us to eliminate possible oscillations of the potential in regions of small internuclear distances. We have found that the functions introduced by Rydberg[31]

$$\rho_{AB}(R_{AB}) = R_{AB} e^{-\beta_{AB}^{(N)} R_{AB}}, \quad (\beta_{AB}^{(N)} > 0), \tag{5}$$

yield high accuracy fits of potential energy curves[32] for diatomic molecules.

The linear parameters c_i, $i=0,1,\ldots,I$ and the nonlinear parameters α and $\beta_{AB}^{(2)}$ are determined by fitting the *ab initio* energies of the diatomic fragments for all the states considered in Eq. (1), computed using the same hydrogen basis set as for the triatomic system and using the same *ab initio* FCI procedure. In Tables I–III we report the parameters corresponding to the diatomic potentials for all the states needed to construct the DIM surface (H_2: $X\ ^1\Sigma_g^+$, H_2^+: $X\ ^2\Sigma_g^+$ and $1\ ^2\Sigma_u^+$). Moreover, it is also feasible to construct higher order DIM matrices by using more diatomic potentials, corresponding to excited states of H_2 and H_2^+, that have been calculated in the preceding section. This possibility has the advantage of a larger initial approximation to the GPES, mainly for the dissociation channels including the long-range behavior, and the disadvantage of a longer time consumed in calculating points of the final GPES.

TABLE II. Two-body[a] term $V^{(2)}(H_2^+,\ ^2\Sigma_g^+)$.

i	c_i
0	0.102 153 115(+01)
1	−0.454 659 563(+00)
2	−0.897 629 388(+00)
3	0.247 689 483(+02)
4	−0.265 726 684(+03)
5	0.172 217 757(+04)
6	−0.659 965 030(+04)
7	0.120 998 241(+05)
8	0.530 127 306(+04)
9	−0.704 964 844(+05)
10	0.125 717 969(+06)
11	−0.763 708 295(+05)
α_{HH^+}	0.167 592 900(+01)
$\beta^{(2)}_{HH^+}$	0.911 150 800(+00)

[a]All the coefficients are given in atomic units.

For the three-body terms of the global potential, $V_{ABC}^{(3)L}$ in Eq. (1), we choose an expansion of order K in product functions that decays exponentially with the distance. Therefore, the $V_{ABC}^{(3)L}$ is neglected at all the dissociation limits and when the internuclear distances tends to zero

$$V_{ABC}^{(3)L}(R_{AB},R_{AC},R_{BC}) = \sum_{ijk}^{K} d_{ijk}^{L} \rho_{AB}^{i} \rho_{AC}^{j} \rho_{BC}^{k}. \tag{6}$$

The variables ρ_{AB}, ρ_{AC}, and ρ_{BC} are the modified form of the Rydberg functions used to represent the long-range term of the two-body potential [see Eq. (5)], but with different exponential parameters

$$\rho_{AB}(R_{AB}) = R_{AB} e^{-\beta_{AB}^{(3)L} R_{AB}}, \quad (\beta_{AB}^{(3)L} > 0). \tag{7}$$

In order to avoid the inclusion of terms that depend on only one interatomic distance in Eq. (7), which have been included in the two-body contributions, one must impose several constraints.[32]

If the system under consideration has three identical atoms, further constraints in the linear d_{ijk}^{L} [Eq. (6)] and nonlinear $\beta_{AB}^{(3)L}$ [Eq. (7)] parameters must be added to ensure that the global potential is invariant with respect to permutations of all the equivalent nuclei.[32]

In Table IV we present the rms values for different fits of the global H_3^+ ground-state potential using one or several three-body terms as indicated by the $LMAX$ value in the corresponding column in this table [see also Eq. (1); in fact, we fit the three-body terms to $V_{H_3^+} - V_{\text{DIM}}$, where $V_{H_3^+}$ are the 8469 calculated data points]. We can see that, when only one three-body term is considered (see $LMAX=1$ column), the accuracy of the fit cannot reach the accuracy of the data points (which we have estimated at about 20 cm^{-1}), even for high order expansions and a great number of linear parameters, the convergence being very slow. The reason for this behavior is that the functional form of the three-body term is unable to reproduce the long-range part of the global potential. However, when the accuracy of the data points is

Downloaded 15 Mar 2013 to 161.111.22.69. Redistribution subject to AIP license or copyright; see http://jcp.aip.org/about/rights_and_permissions

TABLE IV. Accuracy vs the order of the fit.

	$LMAX=1$[a]		$LMAX=2$[a]		$LMAX=3$[a]		$LMAX=4$[a]	
K	n_{par}[b]	rms[c]	n_{par}[b]	rms[c]	n_{par}[b]	rms[c]	n_{par}[b]	rms[c]
3	3	2612.32	6	1311.93	9	509.59	12	453.98
4	6	2536.07	12	352.55	18	217.55	24	115.42
5	10	800.24	20	211.60	30	104.58	40	50.71
6	16	741.13	32	121.71	48	38.47	64	30.85
7	23	397.67	46	83.24	69	27.63	92	18.51
8	32	367.59	64	62.26	96	18.56	128	14.21
9	43	283.65	86	57.01	129	15.04	172	12.45
10	56	265.81	112	51.06	168	12.94	224	10.51
11	71	249.03	142	44.77	213	11.28		
12	89	226.64	178	38.82				
13	109	207.40	218	32.88				
14	132	178.03						
15	158	165.43						
16	187	144.80						
17	219	131.16						

[a]$LMAX$ is the number of nonlinear parameters of the fit.
[b]n_{par} is the number of linear parameters of the fit.
[c]Root-mean-square (rms) errors in cm^{-1}.

yexpected to be greater than 300 cm^{-1} (as usually occurs for the published GPES), this is not an important problem, because with only one three-body term we are able to obtain rms errors lower than the accuracy of the data. In this case we have estimated a better accuracy of the data points. Increasing the number of three-body terms, a better global fit can be reached with much fewer linear parameters. In fact, values of the rms lower than that of the data points can be achieved, as illustrated in Table IV ($LMAX=2,3,4$ columns). We can also see that the convergence is faster in this case. Moreover, when we go from $LMAX=3$ to $LMAX=4$, we can see that, for a given number of linear parameters, we obtain a similar rms indicating that the process is also convergent with respect to the addition of more three-body terms. This result indicates that a linear combination of different three-body terms is able to reproduce the long-range part of the global potential. Therefore, we select as the final fit that underlined in Table IV ($K=8$, $LMAX=3$), corresponding to 96 linear parameters and three nonlinear parameters with an rms value of 18.56 cm^{-1} that is similar to that estimated for the data points. In Table V we collect the parameters corresponding to this ''final'' fit. However, as we can see from Table IV, the procedure presented here is able to attain lower rms errors for the global fit. This is a very important result because if a great number of very accurate data points are obtained,[33] such a procedure would be needed to produce a very accurate analytical GPES. A FORTRAN program to generate the final GPES is available from the authors upon request.[34]

To verify the accuracy of the final GPES we have compared some points with the exact Born–Oppenheimer ones given by Röhse *et al.*[35] The exact energy for dissociation into H_2+H^+ is 37 170 cm^{-1}, just 15 cm^{-1} higher than our potential energy (37 155 cm^{-1}). The exact dissociation limit corresponding to an elongated H_2 $(R=2.50\,a_0)+H^+$ is 54 845 cm^{-1}, just 16 cm^{-1} higher than our potential energy (54 829 cm^{-1}). However, we must stress that the preceding exact value corresponds to the crossing point between the H_2 $(R=2.50\,a_0)+H^+$ and H_2^+ $(R=2.50\,a_0)+H(1s)$ curves, while in our potential we obtain the corresponding crossing point at $R=2.49\,a_0$. Therefore, our dissociation limit (54 711 cm^{-1}) corresponding to an elongated H_2^+ $(R=2.50\,a_0)+H(1s)$ underestimates the exact value given above by 134 cm^{-1}. The exact barrier to linearization is 14 299 cm^{-1}, which is overestimated by our potential by 2 cm^{-1} (14 301 cm^{-1}). Finally, our final GPES underestimates the $H(1s)+H(1s)+H^+$ dissociation energy by about 160 cm^{-1}, corresponding to the region of very high energies (75 301 cm^{-1}).

In Fig. 4 potential energy contours of the H_3^+ ground-state GPES have been plotted using Jacobi coordinates in which $\mathbf{r}$ is the H_2 internuclear vector, $\mathbf{R}$ is the vector joining the center of mass of H_2 to the remaining H, atom and Θ is the angle between them. The GPES corresponding to the present results have been plotted for three different Θ values (0°, 45°, and 90°, see left-hand panels in Fig. 4). We have also plotted, in the right-hand panels of the same figure and for the same Θ angles, the H_3^+ ground-state GPES obtained previously by Prosmiti *et al.*[23] As we can see from the comparison of both GPES in Fig. 4, in both cases the minimum regions, corresponding to short $\mathbf{r}$ and $\mathbf{R}$ distances, are identical. However, if we fix our attention to long $\mathbf{r}$ and $\mathbf{R}$ distances, we can observe two very important differences. The first one is the presence of undesirable structures corresponding to nonsmooth contours that can produce discontinuous derivatives of the Prosmiti *et al.* GPES.[23] The second one is the lack of symmetry produced in the Prosmiti *et al.* GPES,[23] as we can see clearly in the right-hand upper panel in Fig. 4 if we pay attention to the different appearance of the dissociation channels, that should be identical to the present results (see left-hand upper panel in Fig. 4).

Furthermore, in Fig. 5 we have plotted the same GPES as in Fig. 4, but now using a ''stereographic projection'' in hyperspherical coordinates.[36] The three hyperspherical coordinates are ρ, θ, and ϕ_τ.[36] The coordinate ρ can be said to

Downloaded 15 Mar 2013 to 161.111.22.69. Redistribution subject to AIP license or copyright; see http://jcp.aip.org/about/rights_and_permissions

TABLE V. Parameters of the three-body[a] terms $V^{(3)L}$.

	$L=1$	$L=2$	$L=3$
ijk	d^1_{ijk}	d^2_{ijk}	d^3_{ijk}
1 1 0	0.121 717 530(+00)	0.346 021 655(+01)	0.466 629 318(+02)
1 1 1	−0.221 211 994(+01)	−0.907 685 339(+02)	−0.190 559 594(+04)
2 1 0	−0.215 351 596(+01)	−0.123 551 634(+02)	−0.285 432 826(+03)
2 1 1	0.164 527 455(+02)	0.205 302 095(+03)	0.141 983 537(+05)
2 2 0	0.457 345 802(+00)	0.230 134 235(+03)	0.481 335 752(+04)
3 1 0	0.684 755 535(+01)	−0.946 613 730(+01)	−0.378 444 681(+04)
2 2 1	0.323 710 746(+02)	−0.219 021 561(+03)	−0.926 114 214(+05)
3 1 1	−0.107 749 346(+03)	−0.637 342 471(+03)	−0.581 074 306(+05)
3 2 0	−0.403 023 186(+01)	−0.716 554 161(+03)	−0.817 305 389(+04)
4 1 0	0.290 457 775(+01)	0.227 824 886(+03)	0.686 126 620(+05)
2 2 2	0.100 328 131(+03)	0.125 357 893(+04)	0.613 774 043(+06)
3 2 1	−0.784 727 771(+02)	0.676 226 817(+02)	0.234 769 592(+06)
3 3 0	−0.355 883 520(+02)	0.201 090 912(+04)	0.125 170 847(+06)
4 1 1	0.342 774 866(+03)	0.185 046 740(+04)	0.252 158 250(+06)
4 2 0	0.153 901 234(+01)	0.904 243 255(+03)	−0.174 950 585(+06)
5 1 0	−0.507 373 537(+02)	−0.760 782 378(+03)	−0.491 418 372(+06)
3 2 2	−0.781 143 074(+02)	−0.158 269 789(+04)	−0.112 789 831(+07)
3 3 1	0.147 626 200(+03)	0.529 381 639(+03)	−0.488 917 697(+06)
4 2 1	0.366 221 664(+02)	0.175 945 920(+03)	−0.398 080 764(+06)
4 3 0	0.425 337 721(+02)	−0.209 129 837(+04)	−0.153 180 476(+06)
5 1 1	−0.485 699 297(+03)	−0.322 417 947(+04)	−0.828 798 279(+06)
5 2 0	0.376 517 001(+02)	−0.350 892 308(+03)	0.117 875 724(+07)
6 1 0	0.866 519 742(+02)	0.114 901 910(+04)	0.175 662 995(+07)
3 3 2	0.302 965 201(+03)	0.125 881 368(+04)	0.137 477 152(+07)
4 2 2	−0.374 046 089(+03)	0.170 029 500(+03)	0.604 811 338(+06)
4 3 1	−0.115 175 393(+03)	−0.478 735 978(+03)	0.519 369 739(+06)
4 4 0	0.130 307 975(+03)	0.150 614 359(+04)	−0.244 769 673(+06)
5 2 1	0.175 553 953(+03)	0.967 447 169(+02)	0.293 758 736(+06)
5 3 0	−0.138 784 667(+03)	0.441 133 792(+03)	0.153 034 935(+06)
6 1 1	0.163 275 538(+03)	0.209 375 703(+04)	0.136 008 552(+07)
6 2 0	−0.521 422 172(+01)	0.266 104 075(+01)	−0.259 383 146(+07)
7 1 0	−0.457 545 705(+02)	−0.696 999 913(+03)	−0.251 569 755(+07)
$\beta^{(3)L}$	0.652 302 250(+00)	0.868 656 020(+00)	0.218 844 970(+01)

[a]All the coefficients are given in atomic units.

/ describe the overall size of the system, and θ and ϕ_τ describe its shape. Pack and Parker[36] have noted that it is often advantageous to view the surface of the internal sphere as functions of θ and ϕ_τ with ρ fixed. The stereographic projection has X and Y defined as

$$X=\tan\left(\frac{\theta}{2}\right)\cos\phi_\tau, \quad Y=\tan\left(\frac{\theta}{2}\right)\sin\phi_\tau.$$

The three internal coordinates, ρ, θ, and ϕ_τ, are easily related to Jacobi coordinates r_τ, R_τ, and Θ_τ, with $\tau=A,B,C$ (A,B,C denoting the three particles of interest), through the expressions[36]

$$\begin{aligned} R_\tau &= \frac{\rho}{d_\tau\sqrt{2}}\sqrt{1+\sin\theta\cos(2\phi_\tau)}, \\ r_\tau &= \frac{\rho d_\tau}{\sqrt{2}}\sqrt{1-\sin\theta\cos(2\phi_\tau)}, \\ \cos\Theta_\tau &= \frac{\rho}{2}\frac{\sin(2\phi_\tau)\sin\theta}{r_\tau R_\tau}, \end{aligned} \tag{8}$$

with $d_\tau=\sqrt{m_\tau(M-m_\tau)/(\mu M)}$ being the mass-scaling factor, $\mu=\sqrt{m_\tau m_{\tau+1}m_{\tau+2}/M}$ being the reduced mass of the triatomic system, and where $M=m_\tau+m_{\tau+1}+m_{\tau+2}$ is the total mass of the system.

In all panels of Fig. 5, six arrangement channels appear instead of the expected three because of the inversion symmetry in the ϕ_τ coordinate, causing each channel to be repeated twice. Some of the differences and similarities of the present GPES with respect to the Prosmiti *et al.* GPES[23] are more evident from Fig. 5. In this figure we have selected three fixed ρ values. One of them corresponds to the absolute minimum position ($\rho=2.1715\ a_0$), with zero energy represented by the central point in the upper panels of Fig. 5. As we can see from these plots, the minimum region is practically identical and all the dissociation channels are also identical as corresponds to three identical nuclei, for both GPES. However, as we can see in the middle and bottom panels of Fig. 5, when we enlarge the ρ coordinate, a clear breakage of symmetry occurs in the Prosmiti *et al.* GPES[23] (right panels), while the GPES reported herein has the correct symmetry properties (left panels).

IV. ROVIBRATIONAL ANALYSIS AND INFRARED SPECTRA OF THE H_3^+

The infrared spectra of H_3^+ (and its isotopic variants), first observed in 1980 by Oka,[37] have been extensively studied,[23,38–48] and it is nowadays rather well assigned (see, for example, Ref. 48). It should be noted that there are sev-

Downloaded 15 Mar 2013 to 161.111.22.69. Redistribution subject to AIP license or copyright; see http://jcp.aip.org/about/rights_and_permissions

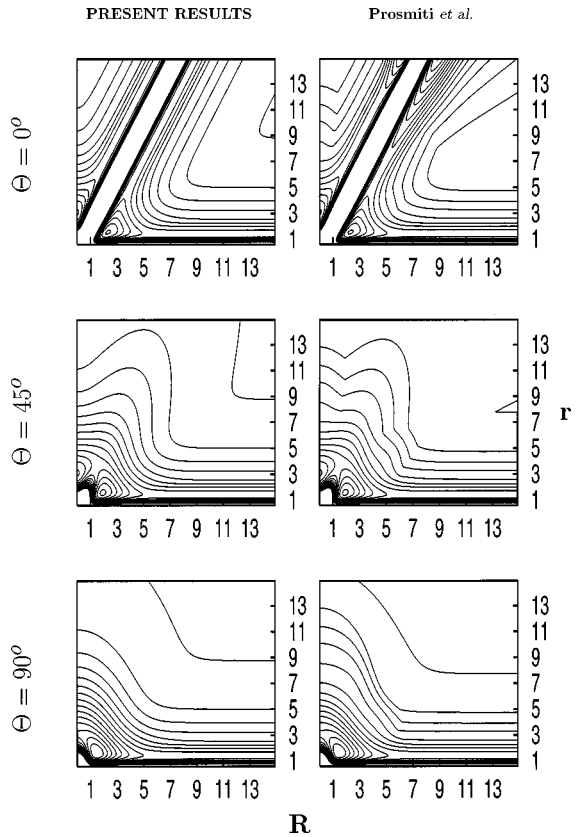

FIG. 4. Contours of the ground-state H_3^+ GPES in Jacobi coordinates **r**, **R**, and **Θ**. For each contour map the **Θ** angle is fixed (0°, upper panels; 45°, intermediate panels, and 90°, bottom panels). The left-hand panels correspond to the present results; the right-hand panels correspond to the Prosmiti *et al.* GPES (Ref. 23). The solid curves are contours of the interaction potential. The contours range from 5000 to 75 000 cm^{-1} for the bottom panels, from 10 000 to 75 000 cm^{-1} for the intermediate panels, and from 15 000 to 75 000 cm^{-1} for the top panels, always in steps of 5000 cm^{-1}. Distances are given in atomic units.

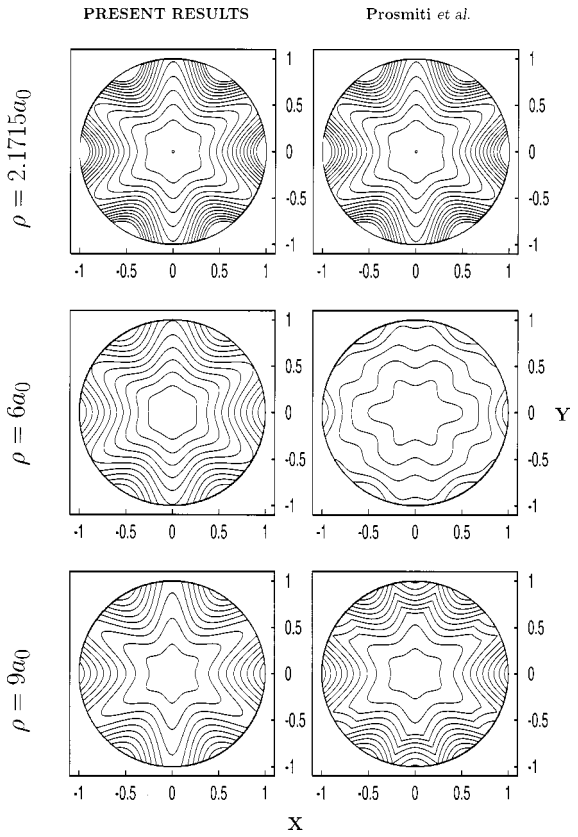

FIG. 5. Stereographic projection of contour plots of the ground-state H_3^+ GPES in hyperspherical coordinates ρ, θ, and ϕ_τ (see the text for more details on these coordinates and for the definition of X and Y). For each contour map the ρ distance is fixed (2.1715 a_0, upper panels; 6 a_0, intermediate panels; and 9 a_0, bottom panels). The left-hand panels correspond to the present results; the right-hand panels correspond to the Prosmiti *et al.* GPES (Ref. 23). The solid curves are contours of the interaction potential. The contours go from 64 000 to 72 000 cm^{-1} for the bottom panels and from 49 000 to 58 000 cm^{-1} for the intermediate panels; in both cases the minimum contours is nearest to the equatorial region and the increment from each contour to the closest one is 1000 cm^{-1}. Finally, for the top panels the contours range from 0 cm^{-1} (the central point in both panels) to 26 000 cm^{-1} in steps of 2000 cm^{-1}.

eral LPES's,[47,48] fitted in the region of the well, which yield results within the experimental resolution, of the order of 0.001 cm^{-1}. However, the potential reported here is designed to describe the entire configuration space, including asymptotic regions as well as the existing conical intersections; this GPES does not have the same spectroscopic accuracy, but a reasonable global accuracy for dynamical calculations. The study of the infrared spectra, which we shall present below, only pretends to check the quality of the GPES presented in this work, in the region of the well, maintaining that we assume a similar accuracy for all the dissociation channels. Moreover, we are also interested in calculating higher rovibrational levels than those previously reported.

The rovibrational energy levels and transitions of H_3^+ have mainly been studied using Jacobi coordinates[23,47–49] and hyperspherical coordinates.[50–55] In this work we shall use the hyperspherical coordinates of Pack and Parker,[56] (denoted by APHJ), which are closely related to those described by Smith[57,58] and Johnson.[59,60] The body-fixed frame chosen corresponds to the principal axis system with the z-axis being perpendicular to the plane of the molecule, and it is related to the space-fixed frame through the α,β,γ Eulerian angles. The three internal coordinates, ρ, θ, and ϕ_τ, are easily related to the Jacobi coordinates r_τ, R_τ, and Θ_τ[36] [see Eq. 8)].

In these coordinates, the Hamiltonian takes the form[56]

$$H = T_\rho + T_h + T_R + T_C + V(\rho,\theta,\phi_\tau), \tag{9}$$

where

$$T_\rho = -\frac{\hbar^2}{2\mu\rho^5}\frac{\partial}{\partial\rho}\rho^5\frac{\partial}{\partial\rho},$$

$$T_h = -\frac{\hbar^2}{2\mu\rho^2}\left[\frac{4}{\sin(2\theta)}\frac{\partial}{\partial\theta}\sin(2\theta)\frac{\partial}{\partial\theta} + \frac{1}{\sin^2\theta}\frac{\partial^2}{\partial\phi_\tau^2}\right], \tag{10}$$

$$T_R = \frac{\hat{J}_x^2}{\mu\rho^2(1-\sin\theta)} + \frac{\hat{J}_y^2}{\mu\rho^2(1+\sin\theta)} + \frac{\hat{J}_z^2}{2\mu\rho^2\sin^2\theta},$$

Downloaded 15 Mar 2013 to 161.111.22.69. Redistribution subject to AIP license or copyright; see http://jcp.aip.org/about/rights_and_permissions

$$T_C = -\frac{i\hbar}{\mu\rho^2}\frac{\cos\theta}{\sin^2\theta}\hat{J}_z\frac{\partial}{\partial\phi_\tau},$$

where $\hat{J}_x, \hat{J}_y, \hat{J}_z$ are the components of the total angular momentum operator in the body-fixed frame.

The eigenstates of this Hamiltonian are expanded as

$$\Phi_i^{JM} = 4\rho^{-5/2}\sum_{v,k,n,\Omega} C_{v,k,n,\Omega}^{JMi} W_{\Omega,n}^{JM}(\alpha,\beta,\gamma,\phi_\tau) \times F_k^{J,\Omega,n}(\theta)\varphi_v(\rho), \tag{11}$$

where the angular functions $W_{\Omega,n}^{JM}$ are of the form

$$W_{\Omega,n}^{JM}(\alpha,\beta,\gamma,\phi_\tau) = \sqrt{\frac{2J+1}{8\pi^2}} D_{M\Omega}^{J*}(\alpha,\beta,\gamma)\frac{e^{in\phi_\tau}}{\sqrt{2\pi}}, \tag{12}$$

the $D_{M\Omega}^{J*}$ being Wigner rotation matrices.[61] In Eq. (11), the $F_k^{J,\Omega,n}(\theta)$ are related to the $G_k(p,q,x)$ Jacobi polynomials[62] as

$$F_k^{J,\Omega,n}(\theta) = \frac{(\sin\theta)^a(\cos\theta)^b}{\sqrt{2}}\sqrt{\frac{(2k+a+b+1)[\Gamma(2k+a+b+1)]^2}{k!\Gamma(k+a+b+1)\Gamma(k+a+1)\Gamma(k+b+1)}}\,G_k(b+1,a+b+1,\cos^2\theta), \tag{13}$$

with $a=|n+\Omega|/2$ and $b=\sqrt{[J(J+1)-\Omega^2]/2}$. This functions are orthonormalized in the interval $0\leqslant\theta\leqslant\pi/2$, $F_k^{J,\Omega,n} = F_k^{J,-\Omega,-n}$ and satisfy

$$\left\{-\frac{4}{\sin(2\theta)}\frac{d}{d\theta}\sin(2\theta)\frac{d}{d\theta} + \frac{n^2+2n\Omega+\Omega^2}{\sin^2\theta} + \frac{2J(J+1)-2\Omega^2}{\cos^2\theta} - \mathcal{K}(\mathcal{K}+4)\right\}F_k^{J,\Omega,n}(\theta), \tag{14}$$

with $\mathcal{K}=4k+2a+2b$.

Finally, the $\varphi_v(\rho)$ functions appearing in Eq. (11) are the solutions of the one-dimensional differential equation

$$\left\{-\frac{\hbar^2}{2\mu}\frac{d^2}{d\rho^2} + V_{\text{ref}}(\rho) - E_v\right\}\varphi_v(\rho) = 0, \tag{15}$$

where $V_{\text{ref}} \equiv V(\rho,\theta=0,\phi_\tau=0)$ in this case. Equation (15) is solved numerically in a large grid of equispaced points in ρ.

The Hamiltonian matrix elements in this basis set representation are of the form

$$\begin{aligned}\langle\Phi_v F_k^{J\Omega n} W_{\Omega n}^{JM}|H|\Phi_{v'}F_{k'}^{J\Omega' n'}W_{\Omega' n'}^{JM}\rangle &= \delta_{\Omega\Omega'}\delta_{nn'}\delta_{kk'}\left\{\langle\varphi_v|-\frac{\hbar^2}{2\mu}\frac{d^2}{d\rho^2}|\varphi_{v'}\rangle + \langle\varphi_v|\frac{\hbar^2}{2\mu\rho^2}|\varphi_{v'}\rangle\left[\frac{15}{4}+\mathcal{K}(\mathcal{K}+4)\right]\right\}\\ &+ \delta_{\Omega\Omega'}\delta_{nn'}\langle\varphi_v|\frac{\hbar^2}{2\mu\rho^2}|\varphi_{v'}\rangle\langle F_k^{J,\Omega,n}|\frac{\cos\theta-1}{\sin^2\theta}|F_{k'}^{J,\Omega,n}\rangle 2n\Omega\\ &+ \delta_{\Omega\Omega'\pm2}\delta_{nn'}\langle\varphi_v|\frac{\hbar^2}{2\mu\rho^2}|\varphi_{v'}\rangle\langle F_k^{J,\Omega,n}|\frac{\sin\theta}{\cos^2\theta}|F_{k'}^{J,\Omega,n}\rangle\\ &\times\sqrt{J(J+1)-\Omega'(\Omega'\pm1)}\sqrt{J(J+1)-(\Omega'\pm1)\Omega}\\ &+ \delta_{\Omega\Omega'}\delta_{n'-n,\lambda}\langle\varphi_v F_k^{J,\Omega,n}|V_\lambda(\rho,\theta)|\varphi_{v'}F_{k'}^{J,\Omega,n'}\rangle,\end{aligned} \tag{16}$$

where the V_λ are the coefficients of the expansion of the potential as

$$V(\rho,\theta,\phi_\tau) = \sum_\lambda V_\lambda(\rho,\theta)e^{i\lambda\phi_\tau} \quad \text{with} \quad \lambda = 0,\pm6,\pm12,\ldots. \tag{17}$$

The integrals involved in the Hamiltonian matrix are evaluated numerically. A trapezoidal integration is used for ρ while the integral on θ is carried out by means of a Gauss–Legendre quadrature with a large number of points ($\approx$300).

The permutational group of three identical particles is isomorphic with the D_3 group and when adding the symmetry under the inversion of spatial coordinates (isomorphic with the C_i group) the group of all symmetry operations becomes isomorphic with the D_{3h} group. Hyperspherical coordinates are particularly well suited for treating the permu-

Downloaded 15 Mar 2013 to 161.111.22.69. Redistribution subject to AIP license or copyright; see http://jcp.aip.org/about/rights_and_permissions

TABLE VI. Rovibrational eigenvalues of H_3^+ for $J=0$ for the present GPES (with zero-point energy, ZPE $=4362.0841\ cm^{-1}$), for the GPES of Ref. 23 (with ZPE$=4362.7801\ cm^{-1}$) and for the LPES of Ref. 7 (with ZPE$=4361.44\ cm^{-1}$). The asterisk mark is used to indicate that we obtain a different assignment than in previous works.

$i(\Gamma,J)$	(v_1,v_2^l)	Γ	Present GPES	GPES of Ref. 23	LPES of Ref. 7	Exp+fit (Ref. 48)
1	$(0,0^0)$	A_1'	0.0000	0.0000	0.00	0.00
2	$(1,0^0))$	A_1'	3179.0807	3178.7480	3178.15	
3	$(0,2^0)$	A_1'	4777.6088	4777.1021	4778.01	
4	$(2,0^0)$	A_1'	6263.5741	6260.4428	6261.81	
5*	$(0,3^3)$	A_1'	7284.4716	7283.1507	7285.32	
6	$(1,2^0)$	A_1'	7769.2711	7766.7933	7768.84	
7	$(0,4^0)$	A_1'	8999.8244	8995.3972	9001.36	
8	$(3,0^0)$	A_1'	9253.9503	9245.7749	9251.42	
9	$(1,3^3)$	A_1'	9967.8366	9963.1895	9968.34	
10	$(2,2^0)$	A_1'	10 593.5900	10 586.2089	10 592.50	
11	$(0,5^3)$	A_1'	10 920.0617	10 910.9288	10 923.49	
12	$(1,4^0)$	A_1'	11 813.2272	11 801.1910	11 814.16	
13	$(4,0^0)$	A_1'	12 149.0286	12 133.5773		
1	$(0,3^3)$	A_2'	7492.4355	7491.4193	7492.61	7493.113
2	$(1,3^3)$	A_2'	10 209.5390	10 206.0906	10 209.65	
3	$(0,5^3)$	A_2'	11 527.6239	11 522.6036	11 529.15	
4	$(2,3^3)$	A_2'	12 831.5467	12 820.0798		
5	$(0,6^3)$	A_2'	13 752.4209	13 739.8937		
1	$(0,1^1)$	E'	2521.0814	2520.9840	2521.20	2521.422
3	$(0,2^2)$	E'	4997.5292	4996.9634	4997.73	4998.058
5	$(1,1^1)$	E'	5554.5911	5554.2073	5553.95	5554.274
7	$(0,3^1)$	E'	7004.9686	7003.2497	7005.81	7006.187
9	$(1,2^2)$	E'	7870.0238	7868.5633	7869.09	7870.664
11	$(2,1^1)$	E'	8488.8693	8485.4081	8487.53	
13	$(0,4^2)$	E'	9111.1184	9107.2931	9112.90	
15	$(1,3^1)$	E'	9652.5387	9649.7530	9653.44	
17	$(0,4^4)$	E'	9996.9482	9990.8078	9996.67	
19	$(2,2^2)$	E'	10 645.3620	10 639.1250	10 644.59	
21*	$(1,4^2)$	E'	10 859.6242		10 862.46	
23	$(3,1^1)$	E'	11 324.3941		11 322.31	
25	$(1,4^2)$	E'	11 656.2449		11 657.69	
27*	$(0,5^1)$	E'	12 077.4622		12 078.43	

tational symmetry of triatomic systems with three identical nuclei, which may yield a significant reduction in the size of the Hamiltonian matrices for a particular irreducible representation. Knowing the effect of the different symmetry operators on the hyperspherical coordinates,[51,63–65] the symmetry adapted basis functions for the Γ irreducible representation of the D_{3h} group are written as linear combination of the functions of Eq. (12) as

$$\mathcal{W}_{\Omega n}^{JM\Gamma}(\alpha,\beta,\gamma,\phi_\tau)=A_{\Omega n}^{J\Gamma}W_{\Omega n}^{JM}+B_{\Omega n}^{J\Gamma}W_{-\Omega -n}^{JM}, \tag{18}$$

where the $A_{\Omega n}^{J\Gamma}$ and $B_{\Omega n}^{J\Gamma}$ coefficients are obtained using the corresponding projection operator, taking the values

$$\begin{aligned} A_{\Omega n}^{J\Gamma} &\propto \{\chi^\Gamma(E)+\chi^\Gamma(E^*)(-1)^\Omega+[\chi^\Gamma(C_3) \\ &\quad +\chi^\Gamma(S_3)(-1)^\Omega]2\cos(4n\pi/3)\}, \\ B_{\Omega n}^{J\Gamma} &\propto [1+2\cos(4n\pi/3)]\{\chi^\Gamma(C_2)(-1)^{J+\Omega+n} \\ &\quad +\chi^\Gamma(\sigma_v)(-1)^{J+n}\} \end{aligned} \tag{19}$$

for $\Omega\neq 0$ and/or $n\neq 0$, while for $n=\Omega=0$ these coefficients are given by

$$\begin{aligned} A_{\Omega n}^{J\Gamma} &\propto \chi^\Gamma(E)+\chi^\Gamma(E^*)+[\chi^\Gamma(C_2)+\chi^\Gamma(\sigma_v)](-1)^J \\ &\quad \times[1+2\cos(4n\pi/3)] \\ &\quad +[\chi^\Gamma(C_3)+\chi^\Gamma(S_3)]2\cos(4n\pi/3), \\ B_{\Omega n}^{J\Gamma} &= 0, \end{aligned} \tag{20}$$

where $\chi^\Gamma(\mathcal{C})$ is the character of the symmetry class $\mathcal{C}$ for the Γ irreducible representation.

The only good quantum numbers associated with each eigenstate are the total angular momentum, J, and the symmetry, characterized by the Γ irreducible representation of the D_{3h} group. Traditionally, for the classification of the eigenstates several approximated quantum numbers are used,[66] (v_1,v_2^l) and G and U. v_1 and v_2 correspond to the symmetric and antisymmetric vibrations, respectively, while l labels the bending. Since in the present treatment the $\varphi_v(\rho)$ functions correspond to a prediagonalization of the symmetric stretch at the equilibrium values of θ and ϕ_τ, v_1 corresponds to the dominant v in the expansion of Eq. (11). The asymmetric stretch, associated with the θ coordinate, is analyzed by comparing the full eigenstates with the monodimensional solutions of the problem for ρ^{eq}, ϕ_τ^{eq} and $J=0$. The l

Downloaded 15 Mar 2013 to 161.111.22.69. Redistribution subject to AIP license or copyright; see http://jcp.aip.org/about/rights_and_permissions

TABLE VII. Root-mean-square (rms) error of the energy levels calculated with the GPES reported in this work with respect to most accurate energy levels of Ref. 48, listing the number of levels used in the statistics as well as the maximum total angular momentum, J_{max}, considered in the comparison.

(v_1, v_2^l)	Number of levels	J_{max}	rms error
$(0, 0^0)$	60	10	0.243
$(0, 1^1)$	122	10	0.261
$(1, 0^0)$	60	10	0.946
$(0, 2^0)$	54	10	0.832
$(0, 2^2)$	105	10	0.474
$(1, 1^1)$	106	10	0.606
$(2, 0^0)$	45	10	1.221
$(0, 3^1)$	71	10	1.227
$(0, 3^3)$	63	10	1.029
$(1, 2^0)$	27	10	0.539
$(1, 2^2)$	47	10	1.414
$(2, 1^1)$	18	10	0.383

is associated with the ϕ_τ variable and is obtained from the dominant n and Ω values, n_{max} and Ω_{max}, respectively, in the expansion of Eq. (11) as $l=|\Omega_{max}+n_{max}|/2$. Similarly, the G number is also obtained from n_{max} and Ω_{max} as $G=|n_{max}+3\Omega_{max}|/2$. Finally, U is equal, in absolute value, to l, and its sign allows us to distinguish between the A_1 and A_2 components. Since we are using symmetry adapted functions, this latter number is not required to specify the character of the states, and in what follows we shall label the states by $(v_1, v_2^l), J, G, \Gamma$. It should be noted that the assignment is not a simple task, especially at high energies, and we have also used the data from previous assignments.[7,48]

In Table VI the eigenvalues for $J=0$ are compared with those of previous works. The LPESs of Refs. 48 and 7 describe the region of the well, yielding results in very good agreement with the experimental transitions, within an error typically less than 0.1 cm^{-1}. However, these LPESs do not correctly describe the asymptotic regions and, therefore, they are not well suited for dynamical studies. The present GPES and that of Ref. 23 describe the entire configuration space and none of them includes adiabatic terms. The spectroscopic accuracy of these two GPES is lower than that of the previously LPES mentioned. However, the present GPES seems to yield results in better agreement with respect to the spectroscopically accurate LPESs of Refs. 48 and 7 than that of Ref. 23. In particular, the maximum difference between the rovibrational levels obtained with this GPES and that of Ref. 7 is of the order of 1–2 cm^{-1} for energies of the order of 16 000 cm^{-1} above the minimum. This difference is considered to be reasonably good for spectroscopy, especially because the adiabatic corrections have not been introduced.

In order to determine more precisely the spectroscopic accuracy of the present GPES, the eigenstates up to $\approx 14\,000$ cm^{-1} have been calculated for total angular momentum in the range $0 \leqslant J \leqslant 20$. The Hamiltonian matrix size increases very rapidly with J and it is therefore impossible to apply a variational method for such large Js. Instead, we use an iterative procedure based on the Lanczos algorithm[67] in two steps. The eigenvalues are obtained with a nonorthogonal Lanczos procedure following the method of Cullum and Willoughby.[68] The eigenstates are then obtained iteratively using the conjugate gradient method[69,70] in a very efficient way. The nuclear spin of the nuclei is 1/2 and the total wave functions, including nuclear spin, must be antisymmetric under exchange of any pair of nuclei, according to the Fermi–Dirac statistic. Following Watson,[66] this implies that the wave function (without the nuclear spin part) must be A_2' or A_2'' for total nuclear spin $I=3/2$ (*ortho* H_3^+) and E' or E'' for $I=1/2$ (*para* H_3^+). Up to $J=10$, the allowed energy levels calculated following this method are in very good agreement with those reported by Dinelli *et al.*,[48] which are of the highest spectroscopic accuracy available for this system; the typical rms deviations for 778 levels with $J \leqslant 10$ are listed in Table VII. As for $J=0$, the typical error is usually lower than 1 cm^{-1} and it should be noted that the larger errors occur for $J>10$ values, as can be seen in Table VIII, where the energy levels for some selected Js are shown together with those of Dinelli *et al.*[48] As noted by Dinelli *et al.*,[48] their calculations for high Js are not well converged, which can be the reason of the discrepancy. However, the method described above allows us the calculation of energy levels for high J values in a very efficient way, and in Table VIII the eigenvalues for $J=15$ and $J=20$ are also shown. Moreover, the use of symmetry adapted functions and hyperspherical coordinates yields a simple and nearly automatic procedure to assign the energy levels, almost always in good agreement with the previous assignment.[48]

Finally, in Table IX, the deviation of the present results with respect to some experimental transitions[41,43,44,46,71,72,73] is shown and compared to that obtained using the levels of Dinelli *et al.*[48] The typical error of the present GPES is of the order of tenths of cm^{-1}. These are larger errors than those obtained by Dinelli *et al.*[48] Nevertheless, it should be noted that in the present potential, of global nature, adiabatic corrections have not been included. As has been recently discussed,[8,74] in order to reproduce the experimental data for H_3^+ to within a few hundredths of cm^{-1} adiabatic corrections to the Born–Oppenheimer approximation should be included, for example using different masses for vibrational and rotational motions.

V. CONCLUSIONS

In this paper we have reported a new global potential energy surface for the ground-state of the H_3^+ system, based on a huge number of full configuration interaction energies, covering all the regions of the potential surface. The rms error of this GPES has been estimated to be lower than 20 cm^{-1}. The global fit is totally symmetric with respect to permutations of the hydrogen atoms and cover all regions of the GPES. To test the quality of this GPES at the absolute minimum region, we have also reported calculations of rovibrational levels up to higher J values than those reported previously and we have reproduced the infrared spectra within 1 cm^{-1} with respect to the experimental ones. We therefore conclude that the accuracy of the present GPES is very high, especially taking into account its ''global character,'' and very well suited for dynamical calculations, due to the accuracy and symmetrical behavior of the dissociation channels.

Downloaded 15 Mar 2013 to 161.111.22.69. Redistribution subject to AIP license or copyright; see http://jcp.aip.org/about/rights_and_permissions

TABLE VIII. Rovibrational eigenvalues (E given in cm^{-1}) of H_3^+ for $J=5,10,15,20$, for the present GPES compared with the very accurate values of Dinelli *et al.* (Ref. 48).

(v_1,v_2^l)	J	G	Γ	E	E (Ref. 48)	(v_1,v_2^l)	J	G	Γ	E	E (Ref. 48)
$(0, 0^0)$	5	0	A_2'	1271.407	1271.269	$(0, 2^2)$	5	7	E''	5363.415	5363.836
$(0, 1^1)$	5	3	A_2'	3553.086	3553.340	$(0, 2^0)$	5	5	E''	5459.792	5460.465
$(0, 1^1)$	5	3	A_2'	3673.833	3673.964	$(0, 2^2)$	5	5	E''	5899.067	5899.400
$(1, 0^0)$	5	0	A_2'	4420.118	4419.147	$(0, 2^0)$	5	1	E''	6002.574	6003.163
$(0, 2^2)$	5	6	A_2'	5658.859	5659.225	$(0, 2^2)$	5	1	E''	6276.403	6276.731
$(0, 2^0)$	5	0	A_2'	6022.482	6023.076	$(0, 2^2)$	5	1	E''	6376.335	6376.537
$(0, 2^2)$	5	0	A_2'	6391.661	6391.893	$(1, 1^1)$	5	4	E''	6410.824	6410.568
$(1, 1^1)$	5	3	A_2'	6568.640	6568.277	$(1, 1^1)$	5	4	E''	6529.765	6529.265
$(1, 1^1)$	5	3	A_2'	6679.769	6679.233	$(1, 1^1)$	5	2	E''	6673.165	6672.774
$(2, 0^0)$	5	0	A_2'	7476.045	7474.726	$(1, 1^1)$	5	2	E''	6793.077	6792.501
$(0, 3^1)$	5	3	A_2'	7962.296	7963.536	$(2, 0^0)$	5	5	E''	6955.032	6953.812
$(0, 3^1)$	5	3	A_2'	8228.598	8229.624	$(2, 0^0)$	5	1	E''	7456.048	7454.731
$(1, 2^2)$	5	6	A_2'	8539.626	8539.900	$(0, 3^3)$	5	8	E''	7637.726	7638.501
$(0, 3^3)$	5	3	A_2'	8682.235	8683.163	$(0, 3^1)$	5	4	E''	7766.665	7767.965
						$(0, 3^1)$	5	4	E''	8052.009	8053.102
$(0, 0^0)$	5	4	E'	929.075	928.975	$(0, 3^1)$	5	2	E''	8089.003	8090.127
$(0, 0^0)$	5	2	E'	1187.237	1187.108	$(1, 2^2)$	5	7	E''	8256.267	8256.630
$(0, 1^1)$	5	5	E'	3299.915	3300.131	$(0, 3^1)$	5	2	E''	8267.694	8269.095
$(0, 1^1)$	5	1	E'	3722.399	3722.638	$(0, 3^3)$	5	2	E''	8396.024	8396.945
$(0, 1^1)$	5	1	E'	3863.331	3863.413	$(0, 3^3)$	5	4	E''	8619.566	8620.290
$(1, 0^0)$	5	4	E'	4085.649	4084.721	$(1, 2^0)$	5	5	E''	8634.387	8634.809
$(1, 0^0)$	5	2	E'	4337.991	4337.030	$(1, 2^2)$	5	5	E''	8774.061	8774.309
$(0, 2^0)$	5	4	E'	5690.234	5690.840	$(0, 3^3)$	5	2	E''	8792.310	8793.047
$(0, 2^0)$	5	2	E'	5939.093	5939.691	$(0, 0^0)$	10	6	A_2'	3726.944	3726.549
$(0, 2^2)$	5	4	E'	6089.518	6089.819	$(0, 1^1)$	10	9	A_2'	5198.084	5198.463
$(0, 2^2)$	5	2	E'	6169.134	6169.466	$(0, 1^1)$	10	9	A_2'	5454.525	5454.531
$(0, 2^2)$	5	2	E'	6327.764	6327.961	$(0, 1^1)$	10	3	A_2'	6539.929	6539.917
$(1, 1^1)$	5	5	E'	6346.639	6346.289	$(0, 2^2)$	10	12	A_2'	6668.748	6671.817
$(1, 1^1)$	5	1	E'	6733.647	6733.247	$(1, 0^0)$	10	6	A_2'	6805.429	6804.443
$(1, 1^1)$	5	1	E'	6860.444	6859.851	$(0, 1^1)$	10	3	A_2'	6959.550	6959.027
$(2, 0^0)$	5	4	E'	7148.211	7146.931	$(1, 1^1)$	10	9	A_2'	8108.049	8109.734
$(2, 0^0)$	5	2	E'	7395.690	7394.378	$(1, 0^0)$	10	6	A_2'	8259.398	8259.969
$(0, 3^1)$	5	5	E'	7829.274	7830.292	$(1, 1^1)$	10	9	A_2'	8445.726	8445.703
$(0, 3^3)$	5	7	E'	7962.996	7963.769	$(0, 2^2)$	10	6	A_2'	8690.943	⋯
$(0, 3^1)$	5	1	E'	8151.162	8152.309	$(0, 2^2)$	10	6	A_2'	9018.072	⋯
$(0, 3^1)$	5	1	E'	8403.942	8404.998	$(0, 2^2)$	10	0	A_2'	9317.968	⋯
$(0, 3^3)$	5	5	E'	8484.773	8485.553	$(1, 2^2)$	10	12	A_2'	9323.874	⋯
$(0, 3^3)$	5	1	E'	8556.215	8557.124	$(0, 2^2)$	10	0	A_2'	9555.467	⋯
$(0, 3^3)$	5	1	E'	8758.187	8759.116	$(1, 2^2)$	10	12	A_2'	9590.213	9598.235
$(1, 2^0)$	5	4	E'	8793.437	8793.787						
$(1, 2^0)$	5	2	E'	8937.686	8938.016	$(0, 0^0)$	10	10	E'	2451.768	2451.609
$(0, 0^0)$	5	3	A_2''	1080.607	1080.490	$(0, 0^0)$	10	8	E'	3197.225	3196.903
$(0, 1^1)$	5	6	A_2''	3047.126	3047.387	$(0, 0^0)$	10	4	E'	4086.839	4086.428
$(0, 1^1)$	5	0	A_2''	3742.949	3743.187	$(0, 0^0)$	10	2	E'	4297.048	4296.621
$(1, 0^0)$	5	3	A_2''	4233.648	4232.699	$(0, 1^1)$	10	11	E'	4539.163	4539.952
$(0, 2^0)$	5	3	A_2''	5829.813	5830.419	$(1, 0^0)$	10	10	E'	5559.543	5559.156
$(0, 2^2)$	5	3	A_2''	5970.939	5971.239	$(0, 1^1)$	10	7	E'	5842.673	5842.782
$(1, 1^1)$	5	6	A_2''	6129.772	6129.561	$(0, 1^1)$	10	7	E'	6145.484	6145.235
$(0, 2^2)$	5	3	A_2''	6213.395	6213.702	$(0, 1^1)$	10	5	E'	6227.051	6226.789
$(1, 1^1)$	5	0	A_2''	6753.528	6753.128	$(0, 1^1)$	10	1	E'	6327.058	6326.432
$(2, 0^0)$	5	3	A_2''	7293.412	7292.111	$(0, 1^1)$	10	5	E'	6628.948	6628.627
$(0, 3^1)$	5	6	A_2''	7551.059	7552.148	$(0, 1^1)$	10	1	E'	6666.099	6666.069
$(0, 3^1)$	5	0	A_2''	8136.357	8137.599	$(0, 2^0)$	10	10	E'	7034.483	7036.309
$(0, 3^3)$	5	6	A_2''	8276.489	8277.121	$(0, 1^1)$	10	1	E'	7055.797	7055.249
$(0, 3^3)$	5	0	A_2''	8650.563	8651.706	$(1, 0^0)$	10	4	E'	7192.905	7191.838
$(1, 2^2)$	5	3	A_2''	8807.236	8808.113	$(1, 0^0)$	10	2	E'	7382.878	7381.697
$(1, 2^0)$	5	3	A_2''	8886.355	8886.702	$(1, 1^1)$	10	11	E'	7474.786	7477.810
						$(0, 2^2)$	10	10	E'	7686.487	7687.224
$(0, 0^0)$	5	5	E''	729.089	729.014	$(0, 2^0)$	10	8	E'	7785.850	7787.014
$(0, 0^0)$	5	1	E''	1250.447	1250.311	$(0, 2^2)$	10	8	E'	8006.069	8006.515
$(0, 1^1)$	5	4	E''	3396.264	3396.538	$(0, 2^2)$	10	8	E'	8443.772	8443.842
$(0, 1^1)$	5	4	E''	3509.980	3510.150	$(0, 0^0)$	10	9	A_2''	2857.013	2856.729
$(0, 1^1)$	5	2	E''	3660.107	3660.349	$(0, 0^0)$	10	3	A_2''	4215.669	4215.239
$(0, 1^1)$	5	2	E''	3792.938	3793.033	$(1, 0^0)$	10	9	A_2''	5945.606	5944.843
$(1, 0^0)$	5	5	E''	3889.573	3888.684	$(0, 1^1)$	10	6	A_2''	6087.601	6087.546
$(1, 0^0)$	5	1	E''	4399.673	4398.704	$(0, 1^1)$	10	6	A_2''	6412.622	6412.298

Downloaded 15 Mar 2013 to 161.111.22.69. Redistribution subject to AIP license or copyright; see http://jcp.aip.org/about/rights_and_permissions

TABLE VIII. (*Continued*.)

(v_1,v_2^l)	J	G	Γ	E	E (Ref. 48)	(v_1,v_2^l)	J	G	Γ	E	E (Ref. 48)
$(0, 1^1)$	10	0	A_2''	7080.879	7080.385	$(0, 0^0)$	15	3	A_2''	8539.756	⋯
$(1, 0^0)$	10	3	A_2''	7317.492	7316.346	$(0, 1^1)$	15	12	A_2''	8773.773	8785.042
$(0, 2^0)$	10	9	A_2''	7506.638	⋯	$(0, 1^1)$	15	12	A_2''	9249.313	⋯
$(0, 2^2)$	10	9	A_2''	8091.794	⋯	$(1, 0^0)$	15	15	A_2''	9470.135	⋯
$(1, 0^0)$	10	3	A_2''	8711.547	⋯	$(0, 1^1)$	15	6	A_2''	10261.999	⋯
$(0, 2^0)$	10	9	A_2''	8932.027	⋯	$(0, 2^2)$	15	15	A_2''	10334.975	⋯
$(1, 1^1)$	10	6	A_2''	9057.381	9057.019	$(2, 0^0)$	15	9	A_2''	10550.716	⋯
$(0, 2^2)$	10	3	A_2''	9268.059	⋯	$(0, 1^1)$	15	0	A_2''	10788.063	⋯
$(1, 1^1)$	10	6	A_2''	9347.706	9347.039	$(0, 3^3)$	15	18	A_2''	10907.195	⋯
$(0, 3^3)$	10	12	A_2''	9403.539	⋯						
$(0, 2^2)$	10	3	A_2''	9564.754	⋯	$(0, 0^0)$	15	13	E''	6154.903	⋯
$(1, 1^1)$	10	0	A_2''	10006.830	⋯	$(0, 0^0)$	15	11	E''	6943.399	⋯
						$(0, 1^1)$	15	16	E''	6954.510	⋯
$(0, 0^0)$	10	7	E''	3485.134	3484.774	$(0, 1^1)$	15	14	E''	7833.973	⋯
$(0, 0^0)$	10	5	E''	3926.570	3926.171	$(0, 0^0)$	15	7	E''	8018.194	⋯
$(0, 0^0)$	10	1	E''	4348.792	4348.363	$(0, 1^1)$	15	14	E''	8267.157	⋯
$(0, 1^1)$	10	10	E''	5026.095	5026.286	$(0, 0^0)$	15	5	E''	8353.640	⋯
$(0, 1^1)$	10	8	E''	5555.350	5555.503	$(0, 0^0)$	15	1	E''	8692.435	⋯
$(0, 1^1)$	10	8	E''	5827.898	5827.729	$(0, 2^2)$	15	17	E''	8918.178	⋯
$(0, 1^1)$	10	4	E''	6401.130	6401.110	$(1, 0^0)$	15	13	E''	9133.420	⋯
$(1, 0^0)$	10	7	E''	6580.702	6579.774	$(0, 1^1)$	15	10	E''	9465.563	⋯
$(0, 1^1)$	10	2	E''	6612.470	6612.443	$(0, 0^0)$	20	18	A_2'	9750.216	⋯
$(0, 1^1)$	10	4	E''	6812.167	6811.731	$(0, 0^0)$	20	18	A_2'	10283.596	⋯
$(1, 0^0)$	10	5	E''	6968.083	6967.289	$(0, 0^0)$	20	12	A_2'	12089.177	⋯
$(0, 1^1)$	10	2	E''	7073.194	7072.408	$(1, 0^0)$	20	18	A_2'	12577.884	⋯
$(0, 2^2)$	10	11	E''	7219.631	7220.652	$(1, 0^0)$	20	18	A_2'	13063.787	⋯
$(1, 0^0)$	10	1	E''	7430.491	7429.303	$(0, 1^1)$	20	21	A_2'	13113.814	⋯
$(0, 1^1)$	10	2	E''	7921.086	⋯	$(0, 0^0)$	20	6	A_2'	13314.547	⋯
$(0, 2^0)$	10	7	E''	8108.997	8109.399	$(0, 0^1)$	20	21	A_2'	13617.513	⋯
$(1, 1^1)$	10	8	E''	8379.827	8380.666						
						$(0, 0^0)$	20	20	E'	8541.217	⋯
$(0, 0^0)$	15	12	A_2'	6575.316	⋯	$(0, 0^0)$	20	16	E'	10700.847	⋯
$(0, 1^1)$	15	15	A_2'	7674.211	⋯	$(0, 1^1)$	20	19	E'	11193.284	⋯
$(0, 0^0)$	15	6	A_2'	8198.855	⋯	$(0, 0^0)$	20	20	E'	11449.958	⋯
$(0, 0^0)$	15	0	A_2'	8705.218	⋯	$(1, 0^0)$	20	20	E'	11490.210	⋯
$(1, 0^0)$	15	12	A_2'	9516.220	⋯	$(0, 1^1)$	20	19	E'	11737.466	⋯
$(0, 1^1)$	15	9	A_2'	9760.939	⋯	$(0, 0^0)$	20	14	E'	12198.864	⋯
$(0, 1^1)$	15	9	A_2'	10308.177	⋯	$(1, 1^1)$	20	19	E'	12220.050	⋯
$(1, 1^1)$	15	15	A_2'	10535.633	⋯	$(0, 0^0)$	20	10	E'	12591.204	⋯
$(0, 1^1)$	15	3	A_2'	10591.474	⋯	$(0, 0^0)$	20	15	A_2''	11112.254	⋯
$(1, 1^1)$	15	15	A_2'	10894.706	⋯	$(0, 1^1)$	20	18	A_2''	11933.578	⋯
						$(0, 1^1)$	20	18	A_2''	12413.818	⋯
$(0, 0^0)$	15	14	E'	5680.067	⋯	$(0, 0^0)$	20	9	A_2''	12803.849	⋯
$(0, 0^0)$	15	10	E'	7268.264	⋯	$(1, 1^1)$	20	18	A_2''	13219.849	⋯
$(0, 0^0)$	15	8	E'	7802.829	⋯	$(0, 0^0)$	20	3	A_2''	13739.397	⋯
$(0, 1^1)$	15	13	E'	8378.518	8385.960	$(1, 1^1)$	20	18	A_2''	13803.937	⋯
$(0, 0^0)$	15	4	E'	8473.833	⋯	$(1, 0^0)$	20	15	A_2''	14135.544	⋯
$(0, 0^0)$	15	2	E'	8655.538	⋯	$(0, 0^0)$	20	19	E''	9284.714	⋯
$(1, 0^0)$	15	14	E'	8693.101	⋯						
$(0, 1^1)$	15	13	E'	8795.509	⋯	$(0, 0^0)$	20	17	E''	10284.461	⋯
$(0, 1^1)$	15	11	E'	9143.916	⋯	$(0, 1^1)$	20	20	E''	11199.609	⋯
$(0, 1^1)$	15	11	E'	9652.220	⋯	$(0, 0^0)$	20	13	E''	11795.800	⋯
$(0, 2^2)$	15	16	E'	9732.107	⋯	$(1, 0^0)$	20	19	E''	12194.310	⋯
$(0, 0^0)$	15	15	A_2''	5092.286	⋯	$(0, 0^0)$	20	11	E''	12354.754	⋯
$(0, 0^0)$	15	9	A_2''	7553.581	⋯	$(0, 0^0)$	20	13	E''	12754.707	⋯
$(1, 0^0)$	15	15	A_2''	8124.367	⋯						

The calculations have also been extended to several excited states using the same spatial conformations (8469 data points for each state). We plan to obtain analytical global potential energy surfaces and rovibrational analysis for excited states of the H_3^+ system using these data and the same procedure presented here for the ground state. Moreover, we plan to study the prototype reaction $H_2^+ + H_2 \rightarrow H_3^+ + H$, for which the present H_3^+ study is a necessary step to obtain the H_4^+ GPES.

Downloaded 15 Mar 2013 to 161.111.22.69. Redistribution subject to AIP license or copyright; see http://jcp.aip.org/about/rights_and_permissions

TABLE IX. Comparison of observed (Refs. 41,43,71,44,46,72, and 73) and calculated transitions (in cm^{-1}) in different absorption bands of H_3^+, for the present calculations and using the energy levels of Ref. 48.

Band	Number of transitions considered	rms error present GPES	rms error Exp+Fit (Ref. 48)
$\nu_2 \leftarrow 0:(0,1^1) \leftarrow (0,0^0)$	92	0.282	0.009
$\nu_1 \leftarrow 0:(1,0^0) \leftarrow (0,0^0)$	9	0.693	0.016
$2\nu_2 l_0 \leftarrow \nu_2:(0,2^0) \leftarrow (0,1^1)$	14	0.371	0.268
$2\nu_2 l_2 \leftarrow \nu_2:(0,2^2) \leftarrow (0,1^1)$	77	0.145	0.008
$\nu_1+\nu_2 \leftarrow \nu_1:(1,1^1) \leftarrow (1,0^0)$	21	0.477	0.009
$\nu_2+\nu_1 \leftarrow \nu_2:(1,1^1) \leftarrow (0,1^1)$	21	0.630	0.125
$3\nu_2 l_1 \leftarrow 0:(0,3^1) \leftarrow (0,0^0)$	15	1.242	0.056

ACKNOWLEDGMENTS

This work has been supported by DGICYT (Ministerio de Educación y Ciencia, Spain) under Grant Nos. PB97-0027 and PB95-0071. We want to acknowledge CCCFC (Universidad Autónoma de Madrid) for the use of a Digital parallel computer.

[1] S. R. Mackenzie and T. P. Softley, J. Chem. Phys. **101**, 10609 (1994).
[2] I. R. McNab, Adv. Chem. Phys. **LXXXIX**, 1 (1995).
[3] J. Tennyson, Rep. Prog. Phys. **57**, 421 (1995).
[4] A. Carrington and R. Kennedy, J. Chem. Phys. **81**, 91 (1984).
[5] D. C. Clary, Annu. Rev. Phys. Chem. **41**, 61 (1990).
[6] J. B. Anderson, J. Chem. Phys. **96**, 3702 (1992).
[7] W. Cencek, J. Rychlewski, R. Jacket, and W. Kutzelnigg, J. Chem. Phys. **108**, 2831 (1998); **108**, 2837 (1998).
[8] O. L. Polyansky and J. Tennyson, J. Chem. Phys. **110**, 5056 (1999).
[9] W. Meyer, P. Botschwina, and P. Burton, J. Chem. Phys. **84**, 891 (1986).
[10] B. M. Dinelli, O. L. Polyansky, and J. Tennyson, J. Chem. Phys. **103**, 10433 (1995).
[11] A. Carrington, D. I. Gammie, J. C. Page, and A. M. Shaw, ''Microwave Spectroscopy of Ionic Complexes at the Dissociation Limit'' in *Molecular Quantum States at Dissociation,* edited by R. Prosmiti, J. Tennyson, and D. C. Clary (CCP6, Daresbury, UK, 1998).
[12] A. Carrington, A. M. Shaw, and S. M. Taylor, J. Chem. Soc., Faraday Trans. **91**, 3725 (1995).
[13] R. Schinke, M. Dupuis, and W. A. Lester, J. Chem. Phys. **72**, 3909 (1980).
[14] A. Ichihara and K. Yokoyama, J. Chem. Phys. **103**, 2109 (1995).
[15] P. E. S. Wormer and F. de Groot, J. Chem. Phys. **90**, 2344 (1989).
[16] A. I. Boothroyd, W. J. Keogh, P. G. Martin, and M. R. Peterson, J. Chem. Phys. **104**, 7139 (1996).
[17] T.-S. Ho, T. Hollebeek, H. Rabitz, L. B. Harding, and G. C. Schatz, J. Chem. Phys. **105**, 10472 (1996).
[18] A. J. Dobbyn and P. J. Knowles, Mol. Phys. **91**, 1107 (1997).
[19] K. Stark and H.-J. Werner, J. Chem. Phys. **104**, 6515 (1996).
[20] A. I. Boothroyd, W. J. Keogh, P. G. Martin, and M. R. Peterson, J. Chem. Phys. **95**, 4343 (1991).
[21] J. R. Henderson and J. Tennyson, Mol. Phys. **89**, 953 (1996).
[22] R. K. Preston and J. C. Tully, J. Chem. Phys. **54**, 4297 (1971).
[23] R. Prosmiti, O. L. Polyansky, and J. Tennyson, Chem. Phys. Lett. **273**, 107 (1997).
[24] A. J. C. Varandas, J. Chem. Phys. **105**, 3524 (1996).
[25] I. Last, M. Gilibert, and M. Baer, J. Chem. Phys. **107**, 1451 (1997).
[26] J. B. Anderson, J. Chem. Phys. **96**, 3702 (1991).
[27] W. Kolos and L. Wolniewicz, J. Chem. Phys. **43**, 2429 (1965); **45**, 509 (1966); **48**, 3672 (1968); Chem. Phys. Lett. **24**, 457 (1974); W. Kolos, K. Szalewicz, and H. J. Monkhorst, J. Chem. Phys. **84**, 3278 (1986); L. Wolniewicz and K. Dressler, *ibid.* **88**, 3861 (1988); **100**, 444 (1994); J. W. Liu and S. Hagstrom, J. Phys. B **27**, 729 (1994); W. Kolos and J. Rychlewski, J. Mol. Spectrosc. **62**, 109 (1976); L. Wolniewicz and K. Dressler, Ber. Bunseuges. Phys. Chem. **99**, 246 (1995); L. Wolniewicz, J. Chem. Phys. **108**, 1499 (1998); T. Detmer, P. Schmelcher, and L. S. Cederbaum, *ibid.* **109**, 9694 (1998).
[28] T. E. Sharp, At. Data **2**, 119 (1971).
[29] H. Partridge, C. W. Bauschlicher, J. R. Stallcop, and E. Levin, J. Chem. Phys. **99**, 5951 (1993).
[30] See EPAPS Document No. E-JCPSA6-008003 for *ab initio* full configuration interaction calculations. This document may be retrieved via the EPAPS homepage (http://www.aip.org/pubservs/epaps.html) or from ftp.aip.org in the directory /epaps/. See the EPAPS homepage for more information.
[31] R. Rydberg, Z. Phys. **73**, 25 (1931).
[32] A. Aguado and M. Paniagua, J. Chem. Phys. **96**, 1265 (1992).
[33] R. Jacket, Private communication (1998).
[34] The authors may be reached by electronic mail at the following address: miguel.paniagua@uam.es
[35] R. Röhse, W. Kutzelnigg, R. Jaquet, and W. Klopper, J. Chem. Phys. **101**, 2231 (1994).
[36] R. T. Pack and G. A. Parker, J. Chem. Phys. **87**, 3888 (1987).
[37] T. Oka, Phys. Rev. Lett. **45**, 531 (1980).
[38] J.-T. Shy, J. W. Farley, W. E. Lamb, Jr., and W. H. Wing, Phys. Rev. Lett. **45**, 535 (1980).
[39] G. D. Carney and R. N. Porter, Phys. Rev. Lett. **45**, 537 (1980).
[40] G. D. Carney, Can. J. Phys. **62**, 1871 (1984).
[41] J. K. G. Watson, S. C. Foster, A. R. W. McKellar, P. Bernath, T. Amano, F. S. Pan, M. W. Crofton, R. S. Altman, and T. Oka, Can. J. Phys. **62**, 1875 (1984).
[42] K. G. Lubic and T. Amano, Can. J. Phys. **62**, 1886 (1984).
[43] M. G. Bawendi, B. D. Rehfuss, and T. Oka, J. Chem. Phys. **93**, 6200 (1990).
[44] L.-W. Xu, M. Rösslein, C. M. Gabrys, and T. Oka, J. Mol. Spectrosc. **153**, 726 (1992).
[45] T. Amano, M.-C. Chan, S. Civis, A. R. W. McKellar, W. A. Majewski, D. Sadovskií, and J. K. G. Watson, Can. J. Phys. **72**, 1007 (1994).
[46] W. A. Majeski, A. R. W. McKellar, D. Sadovskií, and J. K. G. Watson, Can. J. Phys. **72**, 1016 (1994).
[47] R. Jaquet and R. Röhse, Mol. Phys. **84**, 291 (1995).
[48] B. M. Dinelli, L. Neale, O. L. Polyansky, and J. Tennyson, J. Mol. Spectrosc. **181**, 142 (1997).
[49] M. J. Bramley, J. W. Tromp, T. Carrington, Jr., and G. C. Corey, J. Chem. Phys. **100**, 6175 (1994).
[50] R. M. Whitnell and J. C. Light, J. Chem. Phys. **90**, 1774 (1989).
[51] P. Bartlett and B. J. Howard, Mol. Phys. **70**, 1001 (1990).
[52] S. Carter and W. Meyer, J. Chem. Phys. **93**, 8902 (1990).
[53] S. Carter and W. Meyer, J. Chem. Phys. **100**, 2104 (1994).
[54] L. Wolniewicz and J. Hinze, J. Chem. Phys. **101**, 9817 (1994).
[55] J. K. G. Watson, Chem. Phys. **190**, 291 (1995).
[56] R. T. Pack and G. A. Parker, J. Chem. Phys. **90**, 3511 (1989).
[57] F. T. Smith, J. Math. Phys. **3**, 735 (1962).
[58] R. C. Whitten and F. T. Smith, J. Math. Phys. **9**, 1103 (1968).
[59] B. R. Johnson, J. Chem. Phys. **73**, 5051 (1980).
[60] B. R. Johnson, J. Chem. Phys. **79**, 1916 (1983).
[61] R. N. Zare, *Angular Momentum* (Wiley, New York, 1988).
[62] M. Abramowitz and I. A. Segun, *Handbook of Mathematical Functions* (Dover, New York, 1972).
[63] W. Zickendraht, Ann. Phys. (N.Y.) **35**, 18 (1965).
[64] H. Mayer, J. Phys. A **8**, 1562 (1975).
[65] R. M. Whitnell and J. C. Light, J. Chem. Phys. **89**, 3674 (1988).
[66] J. K. G. Watson, J. Mol. Spectrosc. **103**, 350 (1984).
[67] C. Lanczos, J. Res. Natl. Bur. Stand. **45**, 255 (1950).
[68] J. K. Cullum and R. A. Willoughby, *Lanczos Algorithms for Large Symmetric Eigenvalues Computations* (Birkhäuser, Boston, 1985).

Downloaded 15 Mar 2013 to 161.111.22.69. Redistribution subject to AIP license or copyright; see http://jcp.aip.org/about/rights_and_permissions

[69] C.-E. Fröberg, *Numerical Mathematics: Theory and Computer Applications* (Benjamin/Cummings, New York, 1985).
[70] R. E. Wyatt, Adv. Chem. Phys. **LXXIII**, 231 (1989).
[71] S. S. Lee, B. F. Ventrudo, D. T. Cassidy, T. Oka, S. Miller, and J. Tennyson, J. Mol. Spectrosc. **145**, 222 (1991).
[72] D. Uy, C. M. Gabrys, M.-F. Jagod, and T. Oka, J. Chem. Phys. **100**, 6267 (1994).
[73] B. F. Ventrudo, D. T. Cassidy, Z. Y Guo, S. Joo, S. S. Lee, and T. Oka, J. Chem. Phys. **100**, 6263 (1994).
[74] R. Jaquet, Chem. Phys. Lett. **302**, 27 (1999).

Downloaded 15 Mar 2013 to 161.111.22.69. Redistribution subject to AIP license or copyright; see http://jcp.aip.org/about/rights_and_permissions